Electronic Supplementary Material (ESI) for Energy & Environmental Science


# SUPPORTING INFORMATION

## Shape-tailored $TiO_2$ nanocrystals with synergic peculiarities as building blocks for highly efficient multi-stacks dye solar cells

*Luisa De Marco, Michele Manca*, Roberto Giannuzzi, Maria R. Belviso, P. Davide Cozzoli and Giuseppe Gigli*

## Experimental details

*Synthesis of AR4-NRs*: In a typical synthesis,[1] 15 mmol of TTIP was dissolved in 70 g of degassed nonanoic acid and the resulting solution was then reacted with 5 mL of an aqueous 2 M trimethylamine N-oxide solution at 100 °C for 96 h.

*Synthesis of AR16-NRs*: In a typical synthesis,[2] TTIP (17.7 mL, 60 mmol) was added to 50 g of oleic acid at room temperature. Then, the resulting mixture was gradually heated to 270 °C at a rate of about 10°C/min and then kept at this temperature for 2 h.

*Synthesis of BB-NRs*: As a general procedure,[3] 3 g of 1-octadecene, 3 mmol of oleyl amine and 11 mmol of oleic acid were loaded in a three-neck flask and degassed at 120°C for 45 min, after which the mixture is cooled down to 50°C under $N_2$ flow. At this point, 1 mmol of titanium tetrachloride ($TiCl_4$) dissolved in 1 ml of 1-octadecene was added and the flask was heated up to 290°C at a ramp rate of 25°C/min. After heating for 1 h at 290°C, alternated additions of a 0.5 M oleic acid /1-octadecene solution (injected in single portion) and of a 0.5 M $TiCl_4$/1-octadecene solution (delivered at a constant rate of 0.1 mL/min by means of a syringe pump) were performed. The BB-NRs were obtained upon adding an extra 16 mmol of $TiCl_4$ after the primary injection. After the synthesis, the $TiO_2$ nanocrystals were precipitated upon addition of ethanol or 2-propanol:acetone mixtures, separated by centrifugation, and

then washed with acetone to remove the excess surfactant residuals. Then, the resulting products were easily redispersed in an apolar organic solvent, such as toluene or chloroform.

$TiO_2$ paste preparation and DSSC fabrication: nanocrystal suspensions (containing 4% wt/wt of $TiO_2$ as revealed by ICP-AES analysis) were stirred at 60°C for 6 h with ethylcellulose previously dissolved in toluene (10% wt/wt). Then, the solvent exchange was carried out as follows: terpineol was added and the resulting mixture was stirred again for 1 h; finally toluene was removed by a rotary evaporator to obtain pastes suitable for doctor-blade deposition. The paste had the following weight percentage composition: $TiO_2$: 12%; organic capping residuals: 15%; ethylcellulose: 5%; terpineol: 68%. The $TiO_2$ paste was deposited onto F-doped tin oxide conducting glass (15 ohm/sq., provided by Solaronix S.A.). A layer of AR4-NRs based paste was coated on the FTO by doctor blading and gradually heated in oven at air atmosphere; the temperature gradient program had three levels at 170°C (40 min), 350°C (15 min) and 430°C (30 min). This procedure was repeated for AR16-NRs and BB-NRs based paste. The triple-layer NRs-based electrode was finally sintered at 500°C for 30 min. For comparison, double layer commercial nanocrystals-based photoanodes were prepared as follows: a layer of Dyesol 18NR-T paste was deposited onto FTO glass and dried at 125°C for 15 min to obtain a transparent nanocrystalline film of thickness around 12 μm; a scattering layer, ~ 5 μm, made by Dyesol 18-NR-AO colloidal paste was coated onto the transparent layer and the sintering process at 500°C for 30 min was performed. After cooling to 80 °C, the $TiO_2$ electrodes were immersed into a solution 0.2 mM of N719 (provided by Solaronix S.A.) in a mixture of acetonitrile and tert-butyl alcohol (v/v, 1:1), and kept at room temperature for 14 h. The solar cells were assembled by placing a platinum-coated conducting glass (counter electrode) on photoelectrode and sealed with a 50 μm thick Surlyn hot-melt gasket. The redox electrolyte (0.1M LiI, 0.05M $I_2$, 0.6M 1, 2-dimethyl-3-propylimidazolium iodide, and 0.5M tert-butylpyridine

in dried acetonitrile) was introduced into the inter-electrode void space through a hole pre-drilled on the back of the counter electrode.

Nanocrystals and devices characterization: Low-magnification transmission electron microscopy (TEM) images of $TiO_2$ nanocrystals were recorded with a Jeol Jem 1011 microscope operating at an accelerating voltage of 100 kV. The thickness and the active area (0.16 $cm^2$) dimensions of the films were measured with Tencor Alpha-Step 500 Surface Profiler. A Varian Cary 5000 UV–Vis Spectrophotometer was used to measure the diffuse reflectance spectra of the as-prepared films. Scanning electron microscopy (SEM) characterization of $TiO_2$ photoelectrode morphology was performed with a RAITH 150 EBL instrument. Photocurrent-voltage I-V measurements were performed using a Keithley unit (Model 2400 Source Meter). A Newport AM 1.5 Solar Simulator (Model 91160A equipped with a 300W Xenon Arc Lamp) serving as a light source. The light intensity (or radiant power) was calibrated to 100 mW $cm^{-2}$ using as reference a Si solar cell. An aperture 0.25 $cm^2$ mask was applied to the devices before measurements. IPCE measurements were carried out with a computerized setup consisting of a xenon arc lamp (140 W, Newport, 67005) coupled to a monochromator (Cornerstore 260 Oriel 74125). Electrochemical impedance spectroscopy (EIS) was performed by an AUTOLAB PGSTAT 302N (Eco Chemie B.V.) in a frequency range between 300 kHz–30 mHz. The impedance measurements were carried out at different voltage biases in the dark. The resulting impedance spectra were fitted with ZView software (Scribner Associate).

**Table S1.** Photovoltaic parameters recorded for multilayered photoanodes based devices measured upon 0.25 $cm^2$ black mask application under 1 sun illumination (AM 1.5, 100 mW $cm^{-2}$)

| | η % | FF | Voc | Jsc |
|---|---|---|---|---|
| **ML-DSC 10 um (3 AR4 + 7 AR16)** | **8,18** | 0,69 | 0,81 | 14,64 |
| **ML-DSC 14 um (3 AR4 + 4 AR16 + 7 BB)** | **9,40** | 0,69 | 0,81 | 16,81 |
| **ML-DSC 15 um (3 AR4 + 7 AR16 + 5 BB)** | **9,62** | 0,69 | 0,80 | 17,43 |
| **ML-DSC 17 um (7 AR4 + 3 AR16 + 7 BB)** | **9,20** | 0,69 | 0,79 | 16,87 |

**Table S2.** Reproducibility of photovoltaic parameters of DSCs based on multilayered photoanodes and on commercial nanocrystals (Dyesol 18 NR-T + Dyesol 18 NR-AO) under 1 sun illumination (AM 1.5, 100 mW cm-2). PV Characteristics recorded on sensitized 0.16 cm2 electrodes; devices masked with 0.25 cm2 black tape.

| | η % | FF | Voc | Jsc |
|---|---|---|---|---|
| **ML-DSC 17 um (3 AR4 + 7 AR16 + 7 BB) mask 0.25** | 10,47 | 0,69 | 0,81 | 18,73 |
| | 10,38 | 0,70 | 0,81 | 18,30 |
| | 9,96 | 0,71 | 0,80 | 17,54 |
| | 10,26 | 0,70 | 0,81 | 18,10 |
| | 10,10 | 0,68 | 0,80 | 18,57 |
| AVERAGE | **10,23** | **0,70** | **0,81** | **18,25** |

| | η % | FF | Voc | Jsc |
|---|---|---|---|---|
| **D-DSC 17 um (12+5) mask 0.25** | 8,06 | 0,69 | 0,79 | 14,75 |
| | 8,56 | 0,69 | 0,80 | 15,50 |
| | 8,30 | 0,70 | 0,78 | 15,21 |
| | 7,87 | 0,70 | 0,80 | 14,05 |
| | 8,21 | 0,69 | 0,79 | 15,06 |
| AVERAGE | **8,20** | **0,69** | **0,79** | **14,91** |

**Table S3**

Photovoltaic parameters recorded for single layer photoanodes based devices measured upon 0.25 $cm^2$ black mask application under 1 sun illumination (AM 1.5, 100 mW $cm^{-2}$)

| | η % | FF | Voc | Jsc |
|---|---|---|---|---|
| **AR4: 17 um** | **7.24** | 0.69 | 0.76 | 13.82 |
| **AR16: 17 um** | **8.55** | 0.68 | 0.78 | 16.12 |
| **BB: 17 um** | **6.86** | 0.70 | 0.80 | 12.25 |

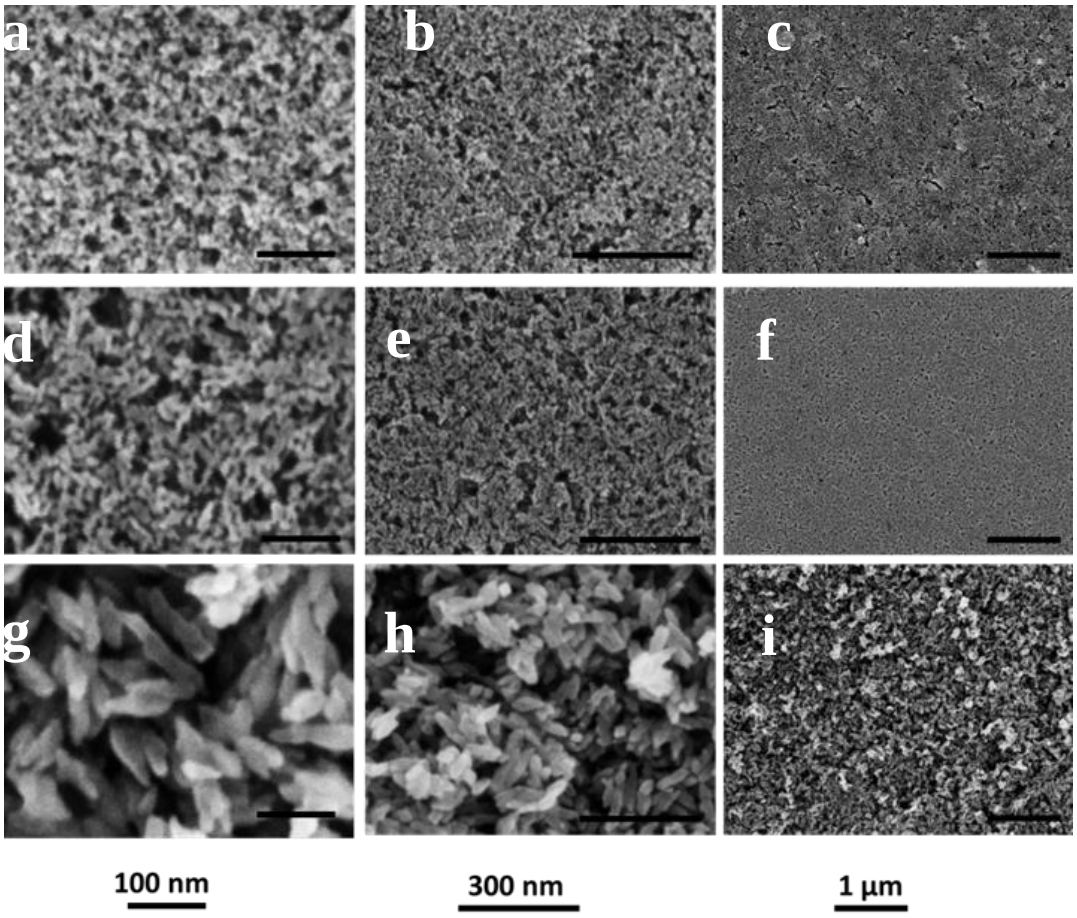


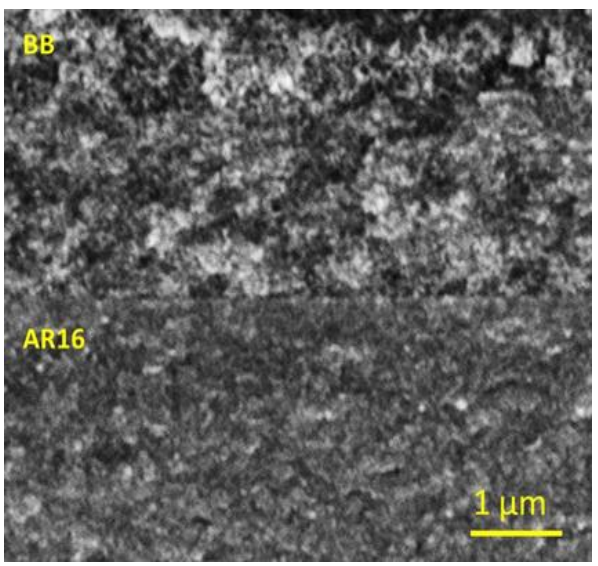


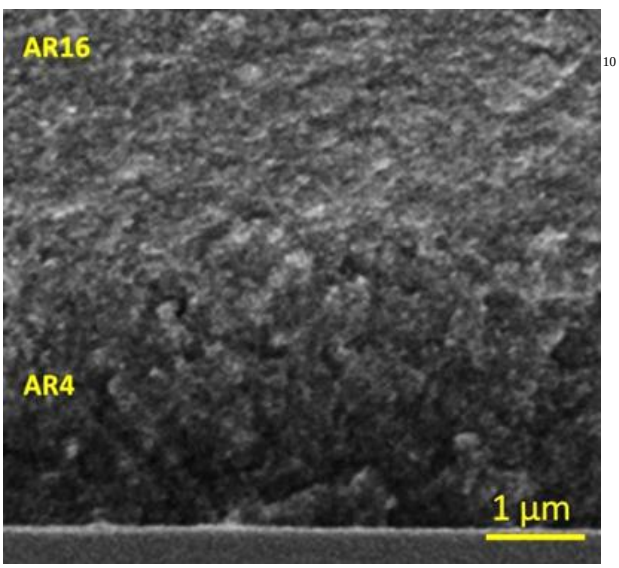


**Figure S1.** SEM images of the sintered films made of AR4-NRs (a, b, c), AR16-NRs (d, e, f) and BB-NRs (g, h, i) and cross sectional view of the engineered three-stack photoelectrode (l, m)

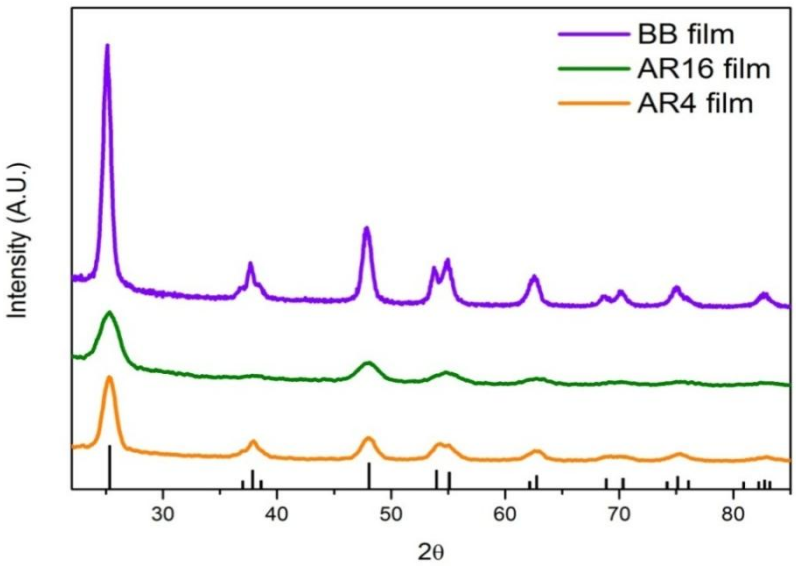


**Figure S2.** XRD patterns of the three of $TiO_2$ NRs-based photoanodes (AR4, AR16 and BB) after high-temperature sintering, along with the reference diffraction lines of bulk $TiO_2$ anatase.

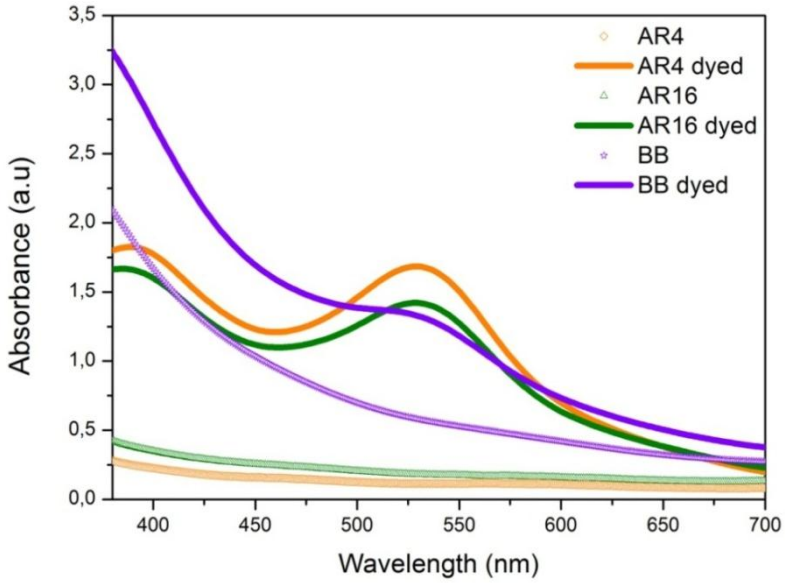


**Figure S3.** UV-vis absorption spectra of 5 μm thick NRs-based photoelectrodes before and after the dye up-taking process.

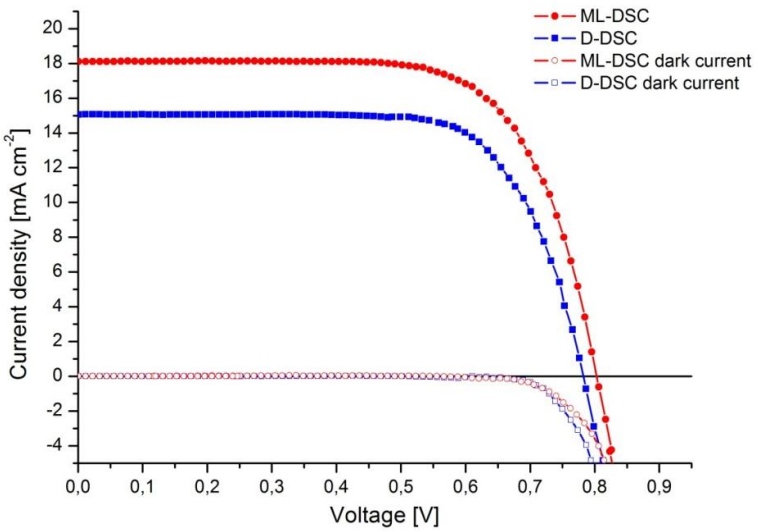


**Figure S4.** Photovoltaic parameters recorded for multilayered photoanodes and Dyesol based devices measured upon 0.25 $cm^2$ black mask application under 1 sun illumination (AM 1.5, 100 mW $cm^{-2}$) and in the dark.

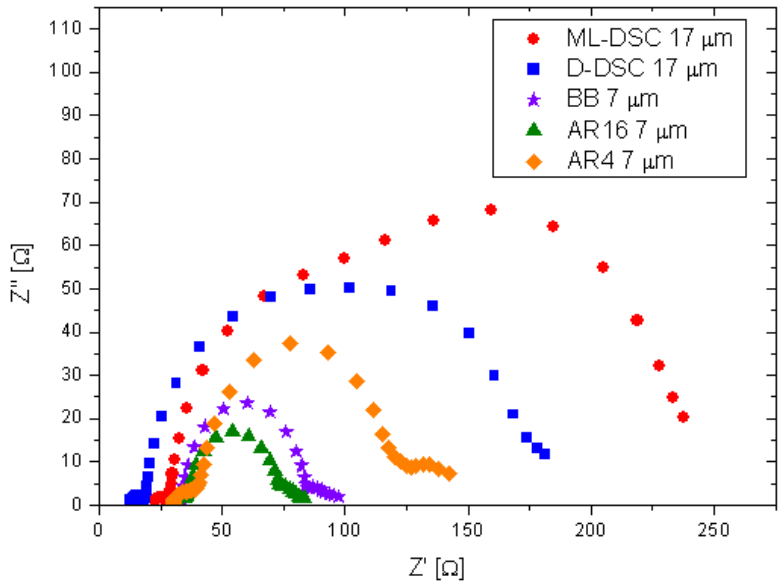


**Figure S5.** Nyquist plots at Voc in dark of DSCs made by five different building-blocks-based PEs

## Calculation procedure of the most relevant electrochemical parameters

Charge recombination can be described by the charge-transfer resistance, $R_{CT}$, which can be obtained from impedance results. In the dark $R_{CT}$ shows an exponential dependence on the bias voltage, which can be satisfactorily described by the expression:[4]

$$R_{CT} = R_0 exp\left(-\beta \frac{eV_{corr}}{k_B T}\right) \quad [1]$$

where $R_0$ is a constant and β is the transfer coefficient, which was calculated according to the model proposed by Bisquert et al. A reaction order (β), typically in the range of 0.5-0.7, is used to provide an empirical description of sublinear recombination kinetics[5] which takes into account the fact that electrons may be transferred from occupied levels located in the energy gap.[5,6] A value of $\beta \approx 0.5$ was extrapolated for all the families of photoelectrodes, which indicated that no noticeable differences in the recombination's reaction order were associable with nanocrystals featured by any particular morphology.

The logarithmic trend of $R_{CT}$ as a function of the corrected bias voltage is reported in Figure S6.

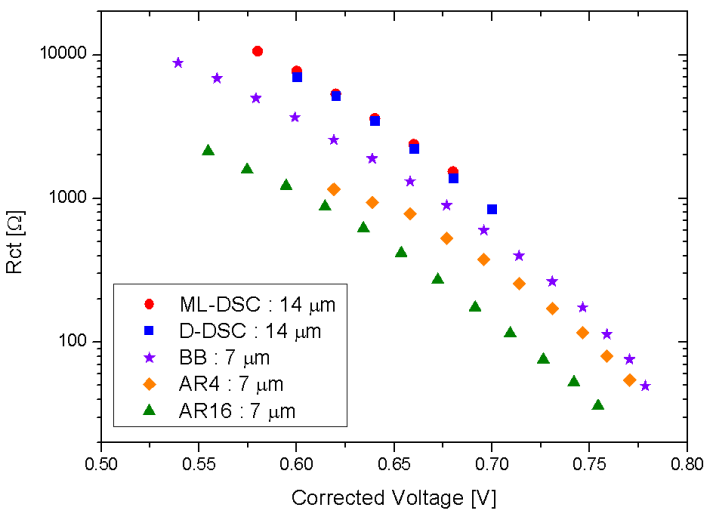


**Figure S6** $R_{CT}$ as a function of the corrected bias voltage

The electron diffusion resistance, $R_T$, shown in Figure S7, decreased exponentially with the corrected voltage. Since the $R_T$ is inversely proportional to the density of electrons at the transport level, it is generally expressed in terms of the Boltzmann distribution:[4]

$$R_T = R_{T_0} exp\left[-\frac{e}{k_B T}\left(V_{corr} + \frac{E_{REDOX} - E_c}{e}\right)\right] \quad [2]$$

where $R_{T0}$ is a constant; as expected, the slope of the semi-logarithmic plot resulted in being the same for all the investigated PEs.

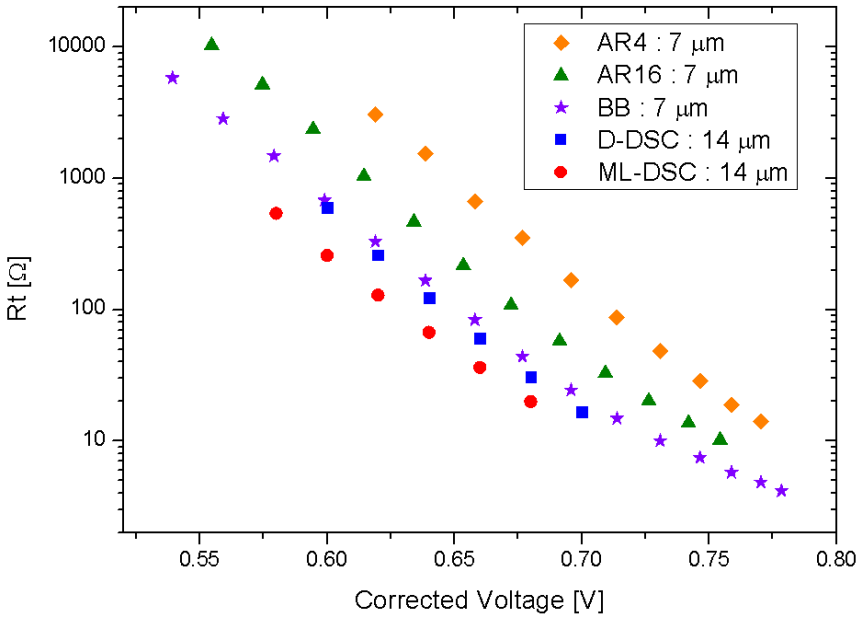


**Figure S7** $R_T$ as a function of the corrected bias voltage

It deserves recalling that the absolute values $R_T$ and $R_{CT}$ are of limited usefulness to the purpose of ranking the performances of different devices. For example, $R_T$ and $R_{CT}$ are both extensive parameters that scale with the overall $TiO_2$ surface area available and additionally depend on the actual number of grain boundaries and lattice defects in the films. As opposed, the $R_{CT}/R_T$ ratio is a more reliable indicator of the genuine electron-collection efficiency of the devices. The competition between the collection and the recombination of electrons can be thus expressed in terms of the electron diffusion length $L_n$. The latter is generally regarded as the most useful parameter to unambiguously compare the electron transport prerogatives of the photoelectrodes.

Nevertheless, it is worthy to emphasize that a rigorous determination of $L_n$ should be performed under specific working conditions.[7]

Coherently with the aim of the present study, the EIS-derived extensive parameters were used to estimate $L_n$ by adopting the quasi-static approximation model proposed by Bisquert et al:[4,8]

$$L_n = d\left(\frac{R_{CT}}{R_T}\right)^{1/2} \quad [3]$$

where *d* is the film thickness.

The electron lifetime $\tau_n$ in dye-sensitized solar cells (DSC) is another central quantity to determine the recombination dynamics in the solar cell.

The kinetics of electron transfer to redox level is usually discussed in terms of the apparent electron lifetime $\tau_n$.[9]

A useful theoretical approach to the electron lifetime, with important practical applications, is to relate $\tau_n$ to equivalent circuit elements that can be separately measured by EIS.

It was thus calculated as $$\tau_n = R_{CT}C_\mu \quad [4]$$

## REFERENCES

[1] L. De Caro, E. Carlino, G. Caputo, P. D. Cozzoli, C. Giannini, *Nat. Nanotechnol*. 2010, **5,** 360.
[2] J. Joo, S. G. Kwon, T. Yu, M. Cho, J. Lee, J. Yoon, T. Hyeon, *J. Phys. Chem. B*, 2005, **109**, 15297
[3] R. Buonsanti, E. Carlino, C. Giannini, D. Altamura, L. De Marco, R. Giannuzzi, M. Manca, G. Gigli, P. D. Cozzoli, *J. Am. Chem. Soc.* 2011, **133**, 19216.
[4] Wang, Q.; Ito, S.; Grätzel, M.; Fabregat-Santiago, F.; Mora-Sero, I.; Bisquert, J.; Bessho, T.; Imai, H. *J. Phys. Chem. B* 2006, **110**, 25210.
[5] Bisquert, J.; Mora-Sero, I. *J. Phys. Chem. Lett.* 2010, **1**, 450.
[6] Villanueva-Cab, J.; Wang, H.; Oskam, G.; Peter, L. M. *J. Phys. Chem. Lett.* 2010, **1**, 748.
[7] Barnes, P. R. F.; O'Regan B. C. *J. Phys. Chem. C*, 2010, **114**, 19134.
[8] J. Bisquert, *J. Phys. Chem. B*, 2002, **106**, 325.
[9] Bisquert, J.; Fabregat-Santiago, F.; Mora-Serò, I.; Garcia-Belmonte, G.; Gimènez, S. *J. Phys. Chem. C*, 2009, **113**, 17278.